Journal of Materials Chemistry C

ROYAL SOCIETY OF CHEMISTRY

PAPER

View Article Online
View Journal | View Issue

Cite this: J. Mater. Chem. C, 2020, 8, 6797

High-efficiency blue photoluminescence in the $Cs_2NaInCl_6:Sb^{3+}$ double perovskite phosphor†

Matthew B. Gray, [a] Shruti Hariyani, [b] T. Amanda Strom, [c] Jackson D. Majher, [a] Jakoah Brgoch [b] and Patrick M. Woodward *[a]

Received 28th February 2020,
Accepted 13th April 2020

DOI: 10.1039/d0tc01037e

rsc.li/materials-c

In this paper, the photoluminescent properties of a lead-free double perovskite $Cs_2NaInCl_6$ doped with Sb^{3+} are explored. The host crystal structure is a cubic double perovskite with $Fm\bar{3}m$ symmetry, a = 10.53344(4) Å, and rock salt ordering of Na^+ and In^{3+}. It is a wide bandgap compound ($E_g \approx 5.1$ eV), and substitution with Sb^{3+} leads to strong absorption in the UV due to localized $5s^2 \rightarrow 5s^15p^1$ transitions on Sb^{3+} centers. Radiative relaxation back to the $5s^2$ ground state, *via* a $^3P_1 \rightarrow {}^1S_0$ transition, leads to intense blue luminescence, centered at 445 nm, with a photoluminescent quantum yield of 79%. The Stokes shift of 0.94 eV is roughly 33% smaller than it is in the related vacancy ordered double perovskite Cs_2SnCl_6. The reduction in Stokes shift is likely due to a change in coordination number of Sb^{3+} from 6-coordinate in $Cs_2NaInCl_6$ to 5-coordinate in Cs_2SnCl_6. In addition to the high quantum yield, $Cs_2NaInCl_6:Sb^{3+}$ exhibits excellent air/moisture stability and can be prepared from solution; these characteristics make it a promising blue phosphor for applications involving near-UV excitation.

Introduction

Main group ions with an ns^2np^0 configuration, like Sb^{3+} and Bi^{3+}, are classic activator ions used in a variety of phosphors and scintillators.[1] The magnitude of the luminescent Stokes shift for these ions can vary greatly depending on the degree of reorganization that occurs in the excited state, which in turn depends upon the structure of the host. When an activator ion is placed on a site that is compressed with respect to its preferred environment, reorganization of the excited state is suppressed, leading to a small Stokes shift. Conversely, if it is placed on a large site, relaxation of the coordination sphere of the activator ion in the excited state can be extensive, resulting in a large Stokes shift. Chloride double perovskites, with the general formula $Cs_2MM'Cl_6$ are favorable phosphor host structures for a variety of luminescent centers, including Mn^{2+}, Yb^{3+}, Eu^{3+}, and Cr^{3+}.[2–8] For example, in a pair of recent reports, Tang *et al.* substituted Sb^{3+} and Bi^{3+} into the vacancy-ordered double perovskite Cs_2SnCl_6, and observed photoluminescence (PL).[9,10] Incorporating up to ~1 mol% of Sb^{3+} produced orange-red light (λ_{max} = 602 nm) with a maximum photoluminescent quantum yield (PLQY) of 37% whereas doping with Bi^{3+} at levels that approach 7 mol% resulted in a blue emission (λ_{max} = 455 nm) with a PLQY as high as 80%. Nanocrystals of $Cs_2SnCl_6:Sb^{3+}$ have also been prepared that show dual emission: a low temperature blue emission (λ_{max} = 438 nm) that disappears upon warming to room temperature and an orange-red emission at 615 nm that is only present when Sb^{3+} is introduced.[11] The quantum efficiency of the nanocrystals is relatively low (PLQY = 8.3%).

The PL characteristics of Sb^{3+} and Bi^{3+} are known to be highly sensitive to their crystallographic environment, but when these ions are doped into Cs_2SnCl_6, the coordination environment is unclear. The aliovalent doping of the trivalent ions for Sn^{4+} requires a compensating charged defect. Recent DFT calculations have suggested the likeliest defect is a chloride vacancy.[10] If the Sb^{3+}/Bi^{3+} ion and the chloride vacancy are located in the same octahedron, it will reduce the coordination environment around the dopant ion from a 6-coordinate octahedron to a 5-coordinate square pyramid. To better understand the structure–property relationships in this class of materials, it would be highly desirable to study a compound where the trivalent ion coordination environment is unambiguous. $Cs_2M^+M^{3+}Cl_6$ double perovskites are an obvious choice because an isovalent substitution for M^{3+} does not require a compensating defect.

Studies of double perovskite hosts have been difficult because many of these compounds have intrinsic moisture instabilities.[12,13] For example, the double perovskites $Cs_2NaMCl_6:Sb^{3+}$ and $Cs_2NaMBr_6:Sb^{3+}$ (M = Sc, Y, La) are incredibly hygroscopic, complicating characterization and limiting potential applications.[12,13] Attempts by Blasse *et al.* to synthesize

[a] Department of Chemistry and Biochemistry, The Ohio State University, 100 W. 18th Avenue, Columbus, Ohio, 43210, USA. E-mail: woodward.55@osu.edu
[b] Department of Chemistry, University of Houston, 3585 Cullen Boulevard, Houston, Texas, 77204, USA
[c] Department of Materials Science, UC Santa Barbara, 2066C Materials Research Lab, Santa Barbara, California, 93106, USA

† Electronic supplementary information (ESI) available. See DOI: 10.1039/d0tc01037e

Cs_2NaSbX_6 (X = Cl, Br) were performed under ultra-dry conditions, but measurements indicated the presence of the thermodynamically stable $Cs_3Sb_2X_9$ phases. While this phase is non-luminescent it could provide a non-radiative decay pathway. It seems that the incorporation of significant amounts of Sb^{3+} rapidly destabilizes most Cs_2NaMX_6 (X = Cl, Br) systems, which necessitates the investigation of alternative host structures.[14,15] Developing a chemically stable double perovskite with an isovalent doping site for the Sb^{3+} cation would alleviate the need for charge compensating chloride vacancy defects, allowing comparative analysis of the effect of coordination number on the photoluminescent properties. This goal led us to study the optical properties of Sb^{3+} ions doped into the lead-free halide double perovskite host $Cs_2NaInCl_6$. Herein, we show that $Cs_2NaInCl_6$:Sb^{3+} is not only useful as a model compound, it is a promising rare-earth free blue phosphor.

Experimental

$Cs_2NaInCl_6$:Sb^{3+} was synthesized by precipitation from an HCl(aq) solution. For a typical synthesis, 20.0 mL of concentrated HCl(aq) (Fisher Scientific, 37%) and 2.0 mL of phosphinic acid (H_3PO_2, Sigma-Aldrich, 50 wt% in H_2O) were heated to 80 °C. Caution should be taken when heating, as phosphinic acid can undergo autoignition upon decomposition into phosphine gas, which occurs near 110 °C. To this solution, 1.00 mmol of In_2O_3 (Alfa Aesar, 99.994%), 2.00 mmol of NaCl (GFS Chemicals, 99%), and varying amounts (0.001–1.00 mmol) of Sb_2O_3 (Acros Organics, 99+%) were added. The solution was heated and stirred to allow the reagents to dissolve. Next, 4.00 mmol of CsCl (Acros Organics, 99+%) was added, immediately triggering the precipitation of $Cs_2NaInCl_6$:Sb^{3+}. This reaction can be described by eqn (1):

$$4CsCl + 2NaCl + In_2O_3 + 6HCl \rightarrow 2Cs_2NaInCl_6 + 3H_2O. \quad (1)$$

The precipitate was then filtered using a porous fritted funnel, washed several times with neat ethanol (Decon Labs Inc., 200 proof), and dried overnight *via* vacuum filtration.

Powder X-ray diffraction (PXRD) data were collected on a Bruker D8 Advance powder diffractometer (40 kV, 40 mA, sealed Cu X-ray tube) equipped with a Lynxeye XE-T position-sensitive detector. The data were collected with an incident beam monochromator (Johansson type SiO_2-crystal) that selects only Cu Kα_1 radiation (λ = 1.5406 Å). Rietveld refinements of laboratory PXRD data were carried out using the TOPAS-Academic (Version 6) software package to determine the crystal structure. Thermogravimetric analysis (TGA) was performed on a Thermogravimetric Analyzer TGA Q50. Samples were heated under a nitrogen stream of 50 mL per minute with a heating rate of 25 °C per minute between 25 °C and 900 °C.

UV-visible diffuse reflectance spectroscopy (DRS) data were collected from 178–890 nm with an Ocean Optics USB4000 spectrometer equipped with a Toshiba TCD1304AP (3648-element linear silicon CCD array). The spectrometer was used with an Ocean Optics DH-2000-BAL deuterium and halogen UV-vis-NIR light source and a 400 μm R400-7-ANGLE-VIS reflectance probe. The detector was calibrated using a Spectralon Diffuse Reflectance Standard.

Steady-state photoluminescence (PL) data were obtained using a Jovin Horiba FluoroMax4 (xenon source, 0.5 nm excitation and emission slit widths, 1 nm step size) equipped with a solid-state sample holder. Luminescent data was analyzed using the FluorEssence (v3.5) software powered by Origin. Temperature-dependent emission spectra were collected by mixing the samples with an optically transparent silicone resin (GE Silicones, RTV615) and depositing the combination onto a quartz slide (Chemglass). Then, using a Janis cryostat (VPF-100) for a temperature-controlled environment from 300–600 K, the emission was measured in 20 K increments (λ_{ex} = 340 nm). Photoluminescent lifetime data was collected using a Horiba DeltaFlex System with a NanoLED N-330 nm (λ_{ex} = 330 nm). Internal photoluminescent quantum yield (PLQY) measurements were performed with a Jovin Horiba FluoroMax4 equipped with a Quanta-φ integrating sphere (15 cm) and a PTFE sample cup. $BaSO_4$ powder dispersed in a silicone resin was used as the blank reference sample. All samples and the blank were excited at 335 nm (λ_{max}) and the absorbance and luminescence signals integrated from 325–345 nm and 370–570 nm, respectively. Radiometric, sphere, and dark count corrections were applied during data acquisition, while corrections for filters and integration time differences were applied in the FluorEssence™ analysis package for Quantum Yield (FluorEssence v3.8.0.60, Origin v8.6001). Additional details are available in the ESI.†

A white light-emitting phosphor-converted light emitting diode (pc-LED) device incorporating the $Cs_2NaInCl_6$:Sb^{3+} phosphor was mixed with lab-made red-emitting $Sr_2Si_5N_8$:Eu^{2+} and commercially available green-emitting β-SiAlON:Eu^{2+} in the same silicon resin mentioned above and cured in a custom brass mold to form a phosphor cap. This cap was placed on a 370 nm LED driven by a 20 mA current, and an AvaSphere-50-IRRAD spectrophotometer was used to obtain the pc-LED luminescence spectrum and performance characteristics.

Results and discussion

Solution precipitation yields single-phase samples characteristic of the double perovskite crystal structure with sharp diffraction peaks (Fig. 1). Analysis indicates that all compounds have $Fm\bar{3}m$ crystal symmetry (Fig. S1, S2 and Table S1, ESI†). The In^{3+} and Na^+ sites are fully ordered in $Cs_2NaInCl_6$, evidenced by the presence of a strong (111) peak at ~14.5° 2θ. The rock salt ordering of octahedral-site cations can be imagined as a three dimensional checkerboard ordering of Na^+ and In^{3+} cations separated by bridging chloride ions. Rietveld refinement yielded bond distances of: d(Cs–Cl) = 3.7271(1) Å, d(Na–Cl) = 2.782(4) Å, and d(In–Cl) = 2.485(4) Å. Sb^{3+} incorporation does not change the average crystal structure, aside from a slight increase in the lattice parameter. Indeed, the lattice parameters increase to 10.54211(8) Å for the highest concentration of Sb^{3+} substitution achieved in a

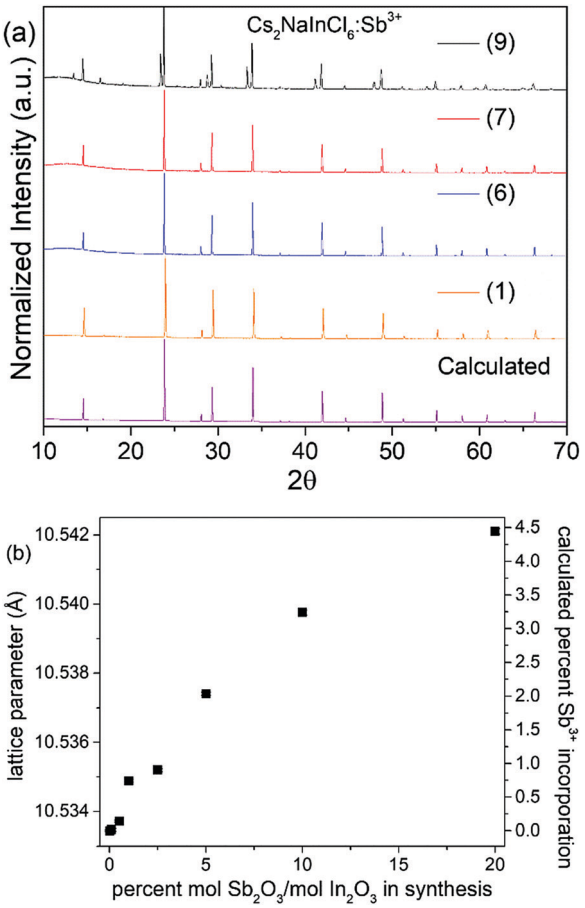

Fig. 1 (a) X-ray powder diffraction patterns of $Cs_2NaInCl_6:Sb^{3+}$ samples with varying amounts of Sb_2O_3 added during synthesis, as well as the calculated diffraction pattern obtained from Rietveld refinement of the Sb-free host. The peaks in samples (1)–(8) can all be accounted for with a cubic double perovskite phase. The additional peaks in sample (9) arise from the presence of $Cs_3Sb_2Cl_9$. (b) The lattice parameter for $Cs_2NaInCl_6:Sb^{3+}$ samples and calculated Sb^{3+} incorporation percentages; the lattice constant error bars are smaller than the symbols.

phase-pure sample compared to 10.53344(4) Å in the undoped $Cs_2NaInCl_6$ sample (Table 1). Although the 6-coordinate Shannon radius of Sb^{3+} (0.90 Å) is slightly smaller than In^{3+} (0.94 Å), the increase in lattice parameter with increased Sb^{3+} content is consistent with the observation that chloride double perovskites with

Table 1 Synthesis details for the $Cs_2NaIn_{1-x}Sb_xCl_6$ samples studied. The Sb^{3+} content, x, was estimated from the lattice parameter, assuming a linear increase as the Sb^{3+} content increases

Sample	$[Sb^{3+}]/[In^{3+}]$ in solution (%)	Lattice parameter (Å)	Nominal Sb content, x
(1)	0.0	10.53344(4)	0.0
(2)	0.1	10.53347(4)	0.0002
(3)	0.5	10.53372(3)	0.0014
(4)	1.0	10.53489(4)	0.0074
(5)	2.5	10.5352(4)	0.009
(6)	5.0	10.53741(5)	0.020
(7)	10.0	10.53976(7)	0.032
(8)	20.0	10.54211(8)	0.044
(9)	50.0	10.5489(3)	0.079

Sb^{3+} have larger lattice parameters than their In^{3+} analogs.[15,16] As shown in previous reports, the amount of Sb^{3+} incorporated into the structure is much smaller than the Sb/In ratio in solution prior to precipitation. This may be related to the hygroscopicity of the Sb^{3+} end-member, $Cs_2NaSbCl_6$.[12–14] Since the full $Cs_2NaIn_{1-x}Sb_xCl_6$ solid solution cannot be prepared, the amount of Sb^{3+} incorporated into the $Cs_2NaInCl_6:Sb^{3+}$ phosphor was estimated using the lattice parameter changes found in the $Cs_2AgIn_{1-x}Sb_xCl_6$ system.[15] In that report, the lattice parameter increased by 0.195 Å as x increased from 0 to 1. If we assume a similar linear increase in the lattice parameter of the $Cs_2NaIn_{1-x}Sb_xCl_6$ solid solution, we can estimate the Sb^{3+} content in these samples (Table 1).

The product remains phase pure until reaching sample (9), where peaks arising from $Cs_3Sb_2Cl_9$ appear in the powder diffraction patterns shown in Fig. 1. Analyzing the thermal stability of the samples by TGA indicates the samples are thermally stable up to 550 °C, as shown in Fig. S3 (ESI†). Increasing the incorporation of Sb^{3+} does not significantly impact the thermal stability; if anything, the thermal stability is slightly enhanced by antimony doping. The samples also did not show any signs of degradation when stored under ambient conditions (room temperature, in air), as evidenced by the lack of changes in the PXRD patterns and optical measurements taken over multiple weeks, (see Fig. S4 and Table S2, ESI†).

The optical properties of the phase-pure samples (1–8) were studied by first analyzing the UV-visible diffuse reflectance spectra (Fig. S5, ESI†). After converting into pseudo-absorbance *via* the Kubelka–Munk function,[17] provided in eqn (2),

$$\alpha = \frac{(1-R)^2}{2R} \quad (2)$$

where α is the optical absorption coefficient, and R is the reflectance, the data were replotted in Fig. 2. The undoped $Cs_2NaInCl_6$ host is a wide bandgap insulator. The band gap is difficult to estimate with a high degree of precision as it occurs

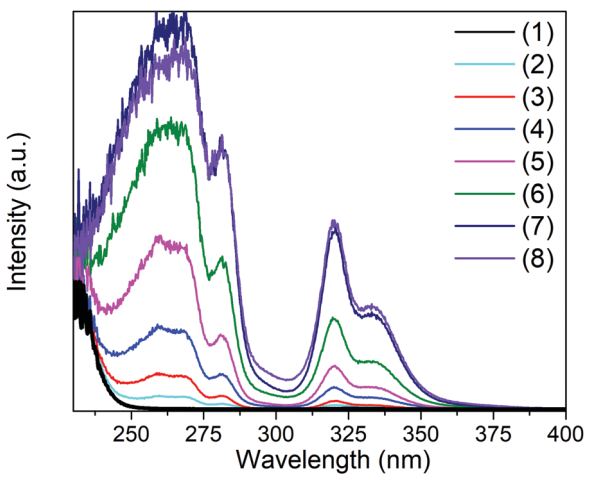

Fig. 2 Pseudo-absorbance obtained from Kubelka–Munk transformation of the diffuse reflectance data of $Cs_2NaInCl_6:Sb^{3+}$ for samples with various concentrations of Sb^{3+}.

near the short wavelength limit of our spectrometer. Extrapolating the upturn in absorbance that occurs below 250 nm, an estimate of $E_g \approx 5.1$ eV (Fig. 2) can be made. Previously reported transmission measurements on single crystals found an upturn of absorbance at a slightly lower energy of 4.8 eV.[18] As soon as Sb^{3+} is incorporated, characteristic $5s^2 \rightarrow 5s^1p^1$ absorption transitions of the $[SbCl_6]^{3-}$ octahedra appear (Fig. 2 and Fig. S6, ESI†). The broad absorption feature centered ~260 nm is assigned as the spin-allowed $^1S_0 \rightarrow {}^1P_1$ transition, and the peak at 280 nm is assigned to the spin and parity forbidden $^1S_0 \rightarrow {}^3P_2$ transition.[12] The transitions at 317 nm and 333 nm can be assigned to the $^1S_0 \rightarrow {}^3P_1$ transition (spin forbidden, parity allowed). This transition is split into two peaks by coupling between the lattice vibrations and empty T_{1u} excited state orbitals; a dynamic Jahn–Teller distortion of the excited state.[5] The intensity of these transitions increases with increasing Sb^{3+} content, corroborating their assignment to absorption from the dopant ion.

Analyzing the photoluminescent excitation spectra provides more information on the electronic structure across this series of compounds (see Fig. 3). The two excitation maxima at 317 nm and 333 nm, which correspond to the Jahn–Teller split $5s^2 \rightarrow 5s^1p^1$ transitions of the $[SbCl_6]^{3-}$ octahedra, lead to the same broad emission. These correspond nicely with the two main absorption features observed in the Kubelka–Munk pseudo-absorption spectra (Fig. 2). The weak excitation observed at 280 nm corresponds to the $^1S_0 \rightarrow {}^3P_2$ transition. Interestingly the relative intensities of the three peaks are quite different in the absorbance and excitation spectra. Not surprisingly, the efficiency of the emission is much higher when both the excitation and emission are associated with the $^1S_0 \rightarrow {}^3P_1$ transitions. The $^1S_0 \rightarrow {}^1P_1$ transition, which produces a strong absorbance at ~260 nm, does not lead to emission. This may be related to its proximity in energy to the band edge, which could allow for thermal excitation into the conduction band and subsequent energy migration. It is also possible that a rapid, radiative return to the ground state (fluorescence) with minimal Stokes shift occurs before crossing over to the triplet excited state.

$Cs_2NaInCl_6$ doped with Sb^{3+} exhibits bright blue photoluminescence (PL), centered at 445 nm with a full-width-at-half-maximum (FWHM) of ~80 nm (0.51 eV) (Fig. 4). As observed in other double perovskites doped with Sb^{3+}, this blue emission can be attributed to local Sb^{3+} excited state relaxation *via* a $^3P_1 \rightarrow {}^1S_0$ pathway. The magnitude of the Stokes shift is indicative of the extent of an excited state reorganization of the $[SbCl_6]^{3-}$ octahedra.[12] The relatively small Stokes shift (0.94 eV) observed in this compound follows a trend observed in other Sb^{3+}-doped double perovskites, which show an increasing Stokes shift with increasing ionic radii of the 6-coordinate 3+ cation (Table 2).[19] The exception is $Cs_2SnCl_6:Sb^{3+}$, where the Stokes shift does not follow the trend extrapolated from the double perovskites. We hypothesize that this is due to the Sb^{3+} adopting a 5-coordinate environment ($[SbCl_5]^{2-}$), which is not surprising given the attraction between the negatively charged Sb'_{Sn} and positively charged $V^{\bullet}_{Cl}$ defects. The stereoactive lone pair of Sb^{3+} makes the square pyramidal geometry more likely than trigonal bipyramidal. The asymmetric coordination environment allows for larger reorganization of the excited state, and thus, a larger Stokes shift.

Analyzing the optical properties of $Cs_2NaInCl_6:Sb^{3+}$ reveals an increase in the Stokes shift as the radius of the trivalent ion that Sb^{3+} replaces increases. While the extent of structural relaxation around the Sb^{3+} dopant is not known, it is reasonable to assume that the antimony ion has more freedom to relax in the excited state as the lattice parameter of the host double perovskite increases, thereby lowering its energy and red shifting the ensuing emission.[1] The emission position in $Cs_2NaInCl_6:Sb^{3+}$ is also independent of the excitation wavelength, indicating that the emission arises from a consistent radiative decay process (Fig. S7, ESI†). The emission characteristics of $Cs_2NaInCl_6:Sb^{3+}$ are similar to the industry standard blue-emitting phosphor, $BaMgAl_{10}O_{17}:Eu^{2+}$ (BAM:Eu^{2+}), which has a 0.90 eV Stokes shift (340 nm excitation, 452 nm emission,

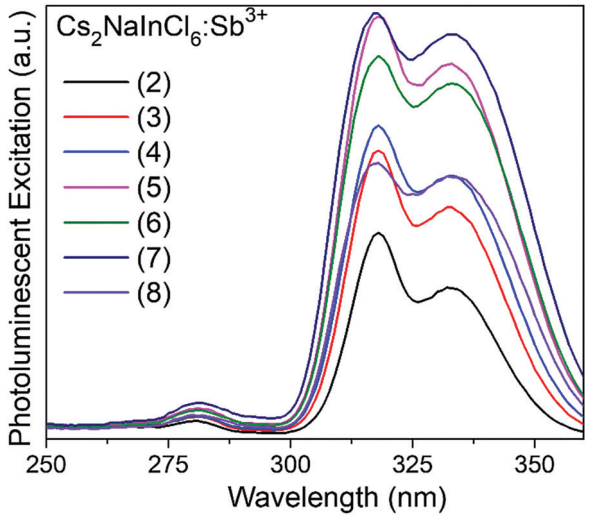

Fig. 3 Excitation spectra of $Cs_2NaInCl_6:Sb^{3+}$ with various concetrations of Sb^{3+}.

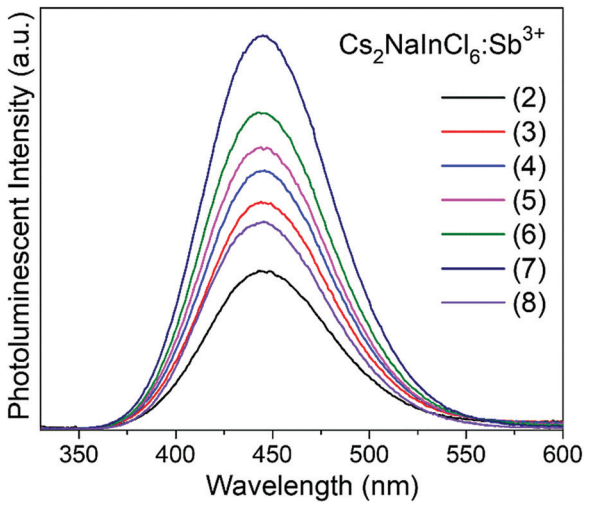

Fig. 4 Emission spectra of $Cs_2NaInCl_6:Sb^{3+}$ samples.

Table 2 Comparison of the Stokes shift in chloride perovskites doped with Sb^{3+}. The energy of the Stokes shift was determined from the maxima of the lowest energy excitation to the maximum of the emission. The ionic radii of the sites onto which Sb^{3+} substitutes were taken from the Shannon 6-coordinate crystal radius[16]

Compound	Stokes shift (eV)	Radius of the host ion (Å)	Host lattice parameter, a (Å)	Ref.
$Cs_2NaScCl_6:Sb^{3+}$	0.93	0.88	10.4875	12 and 14
$Cs_2NaInCl_6:Sb^{3+}$	0.94	0.94	10.5334	This work
$Cs_2NaYCl_6:Sb^{3+}$	1.10	1.04	10.7315	12 and 14
$Cs_2NaLaCl_6:Sb^{3+}$	1.24	1.17	10.9923	12 and 14
$Cs_2SnCl_6:Sb^{3+}$	1.38	0.83	10.3552	9

FWHM = 55 nm).[20] However, the BAM:Eu^{2+} phosphor deteriorates over extended usage due to oxidation of the luminescent center from Eu^{2+} to Eu^{3+}.[21] Not only is this degradation mechanism not operative in the $Cs_2NaInCl_6:Sb^{3+}$ system, the absence of rare-earth ions is an attractive feature.

The maximum emission intensity was observed for the sample (7), corresponding to an approximately 3% substitution of Sb^{3+} for In^{3+}. The slight decrease in luminescence intensity for sample (8) (estimated $[Sb^{3+}] \approx 4\%$), suggests concentration quenching begins to play a role for the higher Sb^{3+} contents. The lower emission intensity of sample (9) can also be attributed in part to the presence of $Cs_3Sb_2Cl_9$. This may give rise to a non-radiative deactivation pathway,[22] not to mention the expected decrease in emission because a non-negligible part of the sample has formed a non-emissive phase. The CIE coordinate diagram (Fig. 5a) for $Cs_2NaInCl_6:Sb^{3+}$ corroborates the expected blue emission, with CIE coordinates of (0.148, 0.067). The PLQY of this compound was determined to be 79(5)% for sample (6), an impressive efficiency for a phosphor prepared from solution (Fig. S8 and Table S3, ESI†).

The thermal stability of the photoluminescence was explored by collecting temperature-dependent PL measurements in 20 K intervals between 300 K and 600 K. These measurements indicate the temperature at which the photoluminescence intensity drops to 50% of its room-temperature value (T_{50}) is 405 K, as shown in Fig. 5b. Minimal shifts were also seen in the emission maximum with temperature, indicating excellent color stability (Fig. S9, ESI†). This is consistent with locally excited systems since the shape of the $[SbCl_6]^{3-}$ octahedra will not significantly change with temperature.

Photoluminescent lifetime measurements were conducted to further understand the decay mechanism. The data plotted in Fig. 5c for sample (6) were fit to a biexponential, following eqn (3), resulting in a lifetime of $\tau_1 = 0.090$ μs accounting for 46% of the decay, and a longer lifetime $\tau_2 = 1.016$ μs accounting for the rest.

$$I = I_0 + A_1 e^{-t/\tau_1} + A_2 e^{-t/\tau_2} \quad (3)$$

These lifetime values are reasonably close to those reported for $Cs_2SnCl_6:Sb^{3+}$ system, which had $\tau_1 = 0.154$ μs and $\tau_2 = 0.821$ μs, where the two lifetimes were attributed to $^3P_1 \rightarrow {}^3P_0$ and $^3P_1 \rightarrow {}^1S_0$ transitions, respectively.[9]

To explore the potential of this phosphor for use in lighting applications, a prototype pc-LED was fabricated by combining a UV-LED chip (λ_{ex} = 370 nm) with a mixture of the $Cs_2NaInCl_6:Sb^{3+}$, a lab prepared red-emitting $Sr_2Si_5N_8:Eu^{2+}$ and a commercially available green-emitting β-SiAlON:Eu^{2+}. The device was driven by a 20 mA current to yield the corresponding emission spectrum plotted in Fig. 5d. The full-spectrum warm white light produced using $Cs_2NaInCl_6:Sb^{3+}$ possess excellent color quality with a color rendering index (R_a)

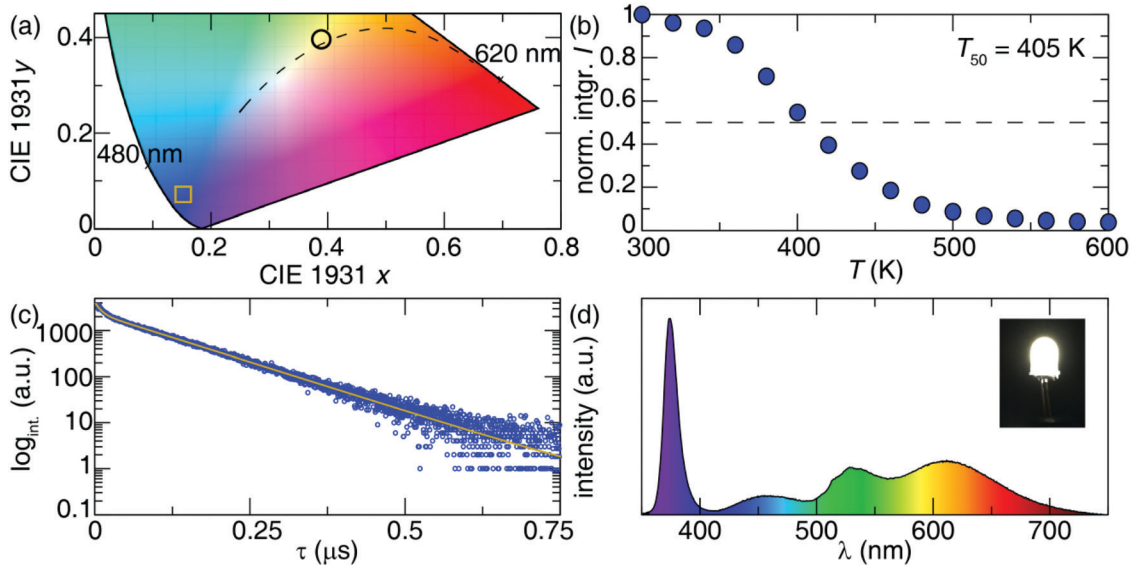

Fig. 5 (a) CIE diagram for $Cs_2NaInCl_6:Sb^{3+}$, where the CIE coordinates (0.148, 0.067) are marked with a square. (b) Normalized, integrated intensity of the emission as a function of temperature. (c) Lifetime measurements of sample (6). (d) The luminescence spectrum of a prototype pc-LED composed of a near UV-LED (λ_{ex} = 370 nm), and three phosphors: $Cs_2NaInCl_6:Sb^{3+}$, $Sr_2Si_5N_8:Eu^{2+}$ and β-SiAlON:Eu^{2+}. The inset is the photograph of the white pc-LED under a forward bias of 20 mA. The circle on the CIE diagram in part (a) shows the CIE coordinates (0.3890, 0.4009) of this pc-LED.

of 90.6, a low correlated color temperature (CCT) of 3972.6 K, and CIE coordinates of (0.3890, 0.4009). To highlight the capability of $Cs_2NaInCl_6$:Sb^{3+} as a blue-emitting phosphor a pc-LED with $BaMgAl_{10}O_{17}$:Eu^{2+}, $Sr_2Si_5N_8$:Eu^{2+} and β-SiAlON:Eu^{2+} was also fabricated. The luminescence spectrum and CIE coordinates of the pc-LED can be seen in Fig. S10 (ESI†).[23] The CIE coordinates of the BAM:Eu^{2+} containing pc-LED closely resembles that of the pc-LED composed of $Cs_2NaInCl_6$:Sb^{3+}, indicating a similar broad band spectrum can be produced from both blue-emitters. The resulting R_a and CCT of the pc-LED using the $BaMgAl_{10}O_{17}$:Eu^{2+} synthesized here is 95.3 and 4479.2 K. The R_a of the BAM:Eu^{2+} containing pc-LED is slightly better; however, the CCT of this device is significantly higher than the pc-LED using $Cs_2NaInCl_6$:Sb^{3+}. The nearly 500 K difference in CCT highlights the ability of $Cs_2NaInCl_6$:Sb^{3+} to be used in conjunction with UV-LEDs to produce a broad spectrum, warm white light.

Based on the results reported here, it could be imagined that a variety of moisture stable double perovskites could successfully host the Sb^{3+} activator in a 6-coordinate environment. To this end, Sb^{3+} was doped into $Cs_2NaBiCl_6$ and $Cs_2AgInCl_6$ hosts using modifications of previously reported synthesis methods.[5,24,25] The samples were each irradiated with light from a broadband Ultra-Violet Products UVSL-25 Mineralight Lamp (365 longwave, 254 shortwave) excitation source to test for luminescence. However, no luminescence is observed at room temperature in $Cs_2NaBiCl_6$ samples doped with Sb^{3+}. The lack of observed luminescence in the Bi^{3+} containing system may arise from the close alignment of the energy levels of Sb^{3+} and Bi^{3+}. These orbitals tend to hybridize efficiently in double perovskites, as demonstrated by the pronounced band gap bowing effect seen in $Cs_2AgBi_{1-x}Sb_xBr_6$ and $Cs_2AgBi_{1-x}Sb_xCl_6$ solid solutions.[26,27] This energetic alignment allows for facile energy transfer between the Sb^{3+} activator and the host, which can enhance concentration quenching. In $Cs_2AgInCl_6$:Sb^{3+}, trace (<1%) amounts of Sb^{3+} lead to an intense yellow-white luminescence, reminiscent of $Cs_2Ag_{0.60}Na_{0.40}InCl_6$:$Bi^{3+}$ or $Cs_2AgIn_{1-x}Bi_xCl_6$ phosphors.[24,28] It appears as though self-trapped excitonic emission leads to the broad photoluminescence observed in both systems. These alternative hosts, while non-toxic and stable, do not have the correct electronic structure to localize the excited state on Sb^{3+}-dopants, illustrating the importance of the host structure in the design of new phosphors.

During the review process, another paper describing photoluminescence in $Cs_2NaInCl_6$:Sb^{3+} appeared in the literature.[29] The photophysical properties reported in both studies are generally in good agreement with each other.

Conclusions

Bright blue luminescence (λ_{max} = 445 nm, FWHM ≈ 0.51 eV) with an internal PLQY of 79(5)% is observed when Sb^{3+} ions are doped into the ordered double perovskite $Cs_2NaInCl_6$ host. In samples precipitated from HCl(aq) solution, approximately 5% of the In^{3+} ions can be replaced with Sb^{3+}, but the PL starts to decrease when the Sb-content gets larger than ~3%. When compared to Cs_2SnCl_6:Sb^{3+} phosphors where the Sb^{3+} ions are likely 5-coordinate, the Stokes shift in $Cs_2NaInCl_6$:Sb^{3+} is smaller (0.94 eV *vs.* 1.38 eV) leading to blue emission rather than orange-red, and the quantum efficiency is more than doubled (79% *vs.* 37%). The emission characteristics of $Cs_2NaInCl_6$:Sb^{3+} phosphors are comparable to the commercial blue phosphor, $BaMgAl_{10}O_{17}$:Eu^{2+} (BAM:Eu^{2+}), which makes it an attractive, rare-earth free alternative to commercial blue phosphors.

Author contributions

The manuscript was written through contributions of all authors. All authors have given approval to the final version of the manuscript.

Conflicts of interest

There are no conflicts of interest to declare.

Acknowledgements

Funding was provided by the National Science Foundation under award number DMR 1610631 (M. B. G., J. D. M., and P. M. W.), DMR 1847701 (S. H. and J. B.) and CER 1911311 (S. H. and J. B.). S. H. and J. B. also thank the Welch Foundation (E-1981) and the Texas Center for Superconductivity at the University of Houston (TcSUH) for supporting this work. PLQY measurements in the MRL Shared Experimental Facilities by A. S. are supported by the MRSEC Program of the NSF under award no. DMR 1720256; a member of the NSF-funded Materials Research Facilities Network (www.mrfn.org). The authors would like to thank David Liu for artistic contributions.

References

1 G. Blasse and B. C. Grabmaier, *Luminescent Materials*, Springer-Verlag, 1994.
2 P. A. Tanner, C. K. Duan, G. Jia and B. M. Cheng, Luminescence of the Elpasolite Series $MI_2MIIMCl_6$ (MI = Cs, Rb; MII = Li, Na; M = Lu, Y, Sc, In) Doped with Europium Using Synchrotron Radiation Excitation, *J. Solid State Chem.*, 2012, **188**, 105.
3 N. Chen, T. Cai, W. Li, K. Hills-Kimball, H. Yang, M. Que, Y. Nagaoka, Z. Liu, D. Yang, A. Dong, C. Y. Xu, R. Zia and O. Chen, Yb-and Mn-Doped Lead-Free Double-Perovskite Cs_2AgBiX_6 (X = Cl^-, Br^-) Nanocrystals, *ACS Appl. Energy Mater.*, 2019, **11**, 16855.
4 Y. Mahor, W. J. Mir, A. Nag and W. J. Mir, Synthesis and Near Infrared Emission of Yb Doped $Cs_2AgInCl_6$ Double Perovskite Microcrystals and Nanocrystals, *J. Phys. Chem. C*, 2019, **123**, 15787.

5 J. D. Majher, M. B. Gray, T. A. Strom and P. M. Woodward, $Cs_2NaBiCl_6$:Mn^{2+}: A New Orange-Red Halide Double Perovskite Phosphor, *Chem. Mater.*, 2019, **31**, 1738.
6 R. Knochenmuss, C. Reber, M. V. Rajasekharan and H. U. Güdel, Broadband Near-Infrared Luminescence of Cr^{3+} in the Elpasolite Lattices $Cs_2NaInCl_6$, Cs_2NaYCl_6, and Cs_2NaYBr_6, *J. Chem. Phys.*, 1986, **85**, 4280.
7 F. Zhao, Z. Song, J. Zhao and Q. Liu, Double Perovskite $Cs_2AgInCl_6$:Cr^{3+}: A Broadband and Near-Infrared Luminescent Materials, *Inorg. Chem. Front.*, 2019, **6**, 3621.
8 G. D. Boyd, H. Kasper, J. H. McFee, L. Bernstein, S. C. Abrahams, F. Lissalde, H. U. Güdel and T. R. Snellgrove, Jahn-Teller Effect in the $^4T_{2g}$ State of Chromium(III) in Dicesium Sodium Indium(III) Hexachloride, *Inorg. Chem.*, 1978, **17**, 1617.
9 J. Li, Z. Tan, M. Hu, C. Chen, J. Luo, S. Li, L. Gao, Z. Xiao, G. Niu and J. Tang, Antimony Doped Cs_2SnCl_6 with Bright and Stable Emission, *Front. Optoelectron.*, 2019, **12**, 352.
10 Z. Tan, J. Li, C. Zhang, Z. Li, Q. Hu, Z. Xiao, T. Kamiya, H. Hosono, G. Niu, E. Lifshitz, Y. Cheng and J. Tang, Highly Efficient Blue-Emitting Bi-Doped Cs_2SnCl_6 Perovskite Variant: Photoluminescence Induced by Impurity Doping, *Adv. Funct. Mater.*, 2018, **28**, 1801131.
11 Y. Jing, Y. Liu, J. Zhao and Z. Xia, Sb^{3+} Doping-Induced Triplet Self-Trapped Excitons Emission in Lead-Free Cs_2SnCl_6 Nanocrystals, *J. Phys. Chem. Lett.*, 2019, **10**, 7439.
12 E. W. J. L. Oomen, W. M. A. Smit and G. Blasse, On the Luminescence of Sb^{3+} in Cs_2NaMCl_6 (with M = Sc, Y, La): A Model System for the Study of Trivalent s2 Ions, *J. Phys. C: Solid State Phys.*, 1986, **19**, 3263.
13 E. W. J. L. Oomen, G. J. Dirksen, W. M. A. Smit and G. Blasse, On the Luminescence of Sb^{3+} in Cs_2NaMBr_6, *J. Phys. C: Solid State Phys.*, 1987, **20**, 1161.
14 E. W. J. L. Oomen, W. M. A. Smit and G. Blasse, The Luminescence of $Cs_2NaSbCl_6$ and $Cs_2NaSbBr_6$: A Transition from a Localized to a Delocalized Excited State, *Chem. Phys. Lett.*, 1987, **138**, 23.
15 T. T. Tran, J. R. Panella, J. R. Chamorro, J. R. Morey and T. M. McQueen, Designing Indirect–Direct Bandgap Transitions in Double Perovskites, *Mater. Horiz.*, 2017, **4**, 688.
16 R. D. Shannon, Revised Effective Ionic Radii and Systematic Studies of Interatomic Distances in Halides and Chalcogenides, *Acta Crystallogr., Sect. A: Cryst. Phys., Diffr., Theor. Gen. Crystallogr.*, 1976, **A32**, 751.
17 M. Kubelka, The Kubelka–Munk Theory of Reflectance, *Zeit. Für Tekn. Physik.*, 1931, 593–602.
18 E. T. McClure, PhD thesis, *Ohio State University*, 2019.
19 X. Wang, W. Meng, W. Liao, J. Wang, R. G. Xiong and Y. Yan, Atomistic Mechanism of Broadband Emission in Metal Halide Perovskites, *J. Phys. Chem. Lett.*, 2019, **10**, 501.
20 A. C. Duke, S. Hariyani and J. Brgoch, $Ba_3Y_2B_6O_{15}$:Ce^{3+} A High Symmetry, Narrow-Emitting Blue Phosphor for Wide-Gamut White Lighting, *Chem. Mater.*, 2018, **30**, 2668.
21 S. Oshio, Mechanism of Luminance Decrease in $BaMgAl_{10}O_{17}$:Eu^{2+} Phosphor by Oxidation, *J. Electrochem. Soc.*, 1998, **145**, 3903.
22 C. W. M. Timmermans, S. O. Cholakh and G. Blasse, The Luminescence of $Cs_3Bi_2Cl_9$ and $Cs_3Sb_2Cl_9$, *J. Solid State Chem.*, 1983, **46**, 222.
23 J. Zhong, Y. Zhuo, S. Hariyani, W. Zhao, J. Wen and J. Brgoch, Closing the Cyan-Gap toward Full Spectrum LED Lighting with $NaMgBO_3$:Ce^{3+}, *Chem. Mater.*, 2020, **32**, 882.
24 J. Luo, X. Wang, S. Li, J. Liu, Y. Guo, G. Niu, L. Yao, Y. Fu, L. Gao, Q. Dong, C. Zhao, L. Leng, F. Ma, W. Liang, L. Wang, S. Jin, J. Han, L. Zhang, J. Etheridge, J. Wang, Y. Yan, E. Sargent and J. Tang, Efficient and Stable Emission of Warm-White Light from Lead-Free Halide Double Perovskites, *Nature*, 2018, **563**, 541.
25 M. B. Gray, E. T. McClure and P. M. Woodward, $Cs_2AgBiBr_{6-x}Cl_x$ Solid Solutions-Band Gap Engineering with Halide Double Perovskites, *J. Mater. Chem. C*, 2019, **7**, 9686.
26 K. Z. Du, W. Meng, X. Wang, Y. Yan and D. B. Mitzi, Bandgap Engineering of Lead-Free Double Perovskite $Cs_2AgBiBr_6$ through Trivalent Metal Alloying, *Angew. Chem., Int. Ed.*, 2017, **56**, 8158.
27 B. Yang, F. Hong, J. Chen, Y. Tang, L. Yang, Y. Sang, X. Xia, J. Guo, H. He, S. Yang, W. Deng and K. Han, Colloidal Synthesis and Charge-Carrier Dynamics of $Cs_2AgSb_{1-y}Bi_yX_6$ (X: Br, Cl; $0 \leq y \leq 1$) Double Perovskite Nanocrystals, *Angew. Chem., Int. Ed.*, 2018, **58**, 2278.
28 M. B. Gray, J. D. Majher, T. A. Strom and P. M. Woodward, Broadband white emission in $Cs_2AgIn_{1-x}Bi_xCl_6$ phosphors, *Inorg. Chem.*, 2019, **58**, 13403.
29 R. Zeng, L. Zhang, Y. Xue, B. Ke, Z. Zhao, D. Huang, Q. Wei, W. Zhou and B. Zou, Highly Efficient Blue Emission from Self-Trapped Excitons in Stable Sb^{3+}-Doped $Cs_2NaInCl_6$ Double Perovskites, *J. Phys. Chem. Lett.*, 2020, **11**, 2053.